Dimitri	Goutaudier	Dimitri.GOUTAUDIER@ensam.eu
First	*Last*	*email*

ASME Paper Title: Parametric Reduced Order Model of a Gas Bearings Supported Rotor

Authors: Dimitri Goutaudier, Jürg Schiffmann, Fabio Nobile

ASME Journal Title: Journal of Engineering for Gas Turbines and Power

Volume/Issue 146(1): 011002 Date of Publication (VOR* Online) October 17, 2023

ASME Digital Collection URL: https://asmedigitalcollection.asme.org/gasturbinespower/article/146/1/011002/1166Reduced-Order-Model-of-a-Gas-Bearings

DOI: https://doi.org/10.1115/1.4063424

*VOR (version of record)

Journal of Engineering for Gas Turbines and Power. Received August 02, 2023;
Accepted manuscript posted September 14, 2023. doi:10.1115/1.4063424

PARAMETRIC REDUCED ORDER MODEL OF A GAS BEARINGS SUPPORTED ROTOR

Dimitri Goutaudier[1,2] Jürg Schiffmann[1], Fabio Nobile[2]

[1]Department of Mechanical Engineering, Laboratory for Applied Mechanical Design, EPFL, Neuchâtel, 2000, Switzerland
[2]Department of Mathematics, Chaire de Calcul Scientifique et Quantification de l'Incertitude, EPFL, Lausanne, 1015, Switzerland
Emails: dimitri.goutaudier@gmail.com, jurg.schiffmann@epfl.ch,fabio.nobile@epfl.ch

ABSTRACT

Gas bearings use pressurized gas as a lubricant to support and guide rotating machinery. These bearings have a number of advantages over traditional lubricated bearings, including higher efficiency in a variety of applications and reduced maintenance requirements. However, they are more complex to operate and exhibit nonlinear behaviors. This paper presents a parametric hyper Reduced Order Model (h-ROM) of a gas bearings supported rotor enabling to speed up the computations up to a factor 100 while preserving satisfactory accuracy. A Galerkin projection setting is employed to reduce the dimension of the governing equations and the nonlinear terms are efficiently tackled with a sparse sampling technique. The performances of the h-ROM are compared to a high fidelity model both in terms of accuracy and computation time, demonstrating the potential for future anomaly detection applications.

Keywords: gas bearings, dynamical system, reduced order model, parametric adaptation

1. INTRODUCTION

Real-time simulation of gas bearings supported turbomachinery could force a breakthrough in smart monitoring with physically interpretable anomaly detection techniques. In contrast to purely data-driven predictive maintenance frameworks [1], the ultimate goal of this research work is to monitor a complex dynamical system with an accurate physics-based surrogate model, empowered with data assimilation techniques only where needed. This is the so-called hybrid twin paradigm gaining more and more importance in a variety of mechanical engineering applications [2]. We focus herein on the first step toward a hybrid twin, that is the development of a surrogate model directly based on the governing equations of the dynamical system. In this study, a major scientific challenge is the real-time simulation of gas bearings supported rotors that may operate at extremely high speeds to maximize their performances.

Projection-based model order reduction is a promising framework to perform fast simulations accounting for nonlinear behaviors while preserving satisfactory accuracy [3]. In this context, Galerkin projection settings have been successfully employed in a variety of situations. The idea is to project the governing equations of the dynamical system onto a low dimensional linear subspace, and to approximate the system's state variables in this same subspace. In many situations, it is indeed observed that the numerical solution of a problem, seemingly evolving in a high dimensional space related to some fine spatial discretization, can often be described with a reduced number of degrees of freedom. An established method to identify a suitable low dimensional subspace is the Proper Orthogonal Decomposition (POD) combined with the method of snapshots [4, 5]. It extracts the most energetic dynamical modes of the system from snapshots of the true solution picked at different times of the physical problem. However, even if a Galerkin projection setting reduces the number of unknowns, the evaluation of a projected nonlinear term might still be too expensive to evaluate. It then becomes necessary to tackle the nonlinear terms with a dedicated technique based on sparse sampling. Several methods are available such as the MPE [6], the GNAT [7] or the DEIM methods [8]. Such a surrogate model is referred as a hyper-reduced order model (h-ROM) in the scientific litterature.

An additional difficulty arises when it comes to predict the response of a system to various inputs, such as external loads or changes in operating conditions. Indeed, a projection-based reduced order model is by construction obtained from snapshots of the solution computed with a high fidelity model at user-selected values of the system's parameters (training points). Consequently, the reduced order model is not expected to provide accurate predictions away from these training points. Common approaches to solve this problem are the construction of a global reduced basis with the concatenation method [3], the clustering of the parameter space with multiple local bases [9, 10], and dedicated interpolation techniques resorting to differential geometry to preserve the structure of a basis [11, 12]. To the best of the authors knowledge, this study presents the first application of a hyper reduced order modelling framework to a gas bearings dynamical system. Other model reduction approaches have been studied on similar technologies in [13–15].

Journal of Engineering for Gas Turbines and Power. Received August 02, 2023;
Accepted manuscript posted September 14, 2023. doi:10.1115/1.4063424

This paper is organized as follows. In section 2 we present the governing equations of a rigid rotor supported by two gas-lubricated Herringbone Grooved Journal Bearings (HGJB). In section 3 we present our methodology to derive a computationally efficient hyper-reduced order model (h-ROM). In section 4 we briefly present the method employed to adapt the reduced bases of the h-ROM to any rotor speed and compressibility number in user-defined ranges of interest. In section 5 we compare the performances of the developed h-ROM with a high fidelity model, both in terms of accuracy and computation time. Last, in section 6 we present the main limitations of the proposed framework.

2. GOVERNING EQUATIONS

The studied system consists in a rotor supported by two gas-lubricated Herringbone Grooved Journal Bearings (HGJB). The gas inside the bearings is dragged by the rotative motion of the rotor and accumulates near the locations with smallest clearance, generating a repulsive aerodynamic force with an inward normal component, see Figure 1.

We assume that the two bearings are fixed, identical and perfectly aligned. The rotor is modelled as a rigid body with four degrees of freedom chosen to be the x, y coordinates of its geometrical center and the tilting angles in the $(y, z)-$ and $(z, x)-$planes. The forces acting on the rotor are its weight, the total aerodynamic force, and an imbalance force due a mismatch between the inertial and geometrical axes of the rotor. Using the same non-dimensional parameters as in [16], the rotor-dynamics equations in the fixed reference frame of the bushings are given by:

$$\begin{aligned} \bar{m}_r \ddot{\epsilon}_x &= \bar{m}_r \bar{g} + \bar{F}_x^1 + \bar{F}_x^2 + \bar{F}_{x\_im}^1 + \bar{F}_{x\_im}^2 \\ \bar{m}_r \ddot{\epsilon}_y &= \bar{F}_y^1 + \bar{F}_y^2 + \bar{F}_{y\_im}^1 + \bar{F}_{y\_im}^2 \\ \bar{I}_T \ddot{\zeta} + \bar{I}_P \dot{\phi} &= \bar{F}_y^1 \bar{l}_1 - \bar{F}_y^2 \bar{l}_2 + \bar{M}_{\zeta\_im} \\ \bar{I}_T \ddot{\phi} - \bar{I}_P \dot{\zeta} &= -\bar{F}_x^1 \bar{l}_1 + \bar{F}_x^2 \bar{l}_2 + \bar{M}_{\phi\_im} \end{aligned} \tag{1}$$

where $\bar{F}_x^i, \bar{F}_y^i$ are the components of the non-dimensional aerodynamic force generated in bearing $i = 1, 2$. The available clearance between the rotor and the bushings being negligible compared to the rotor's length, the pressure distribution can be assumed symmetrical about the bearing mid-planes. The aerodynamic force generated in bearing $i = 1, 2$ is then given by:

$$\begin{bmatrix} \bar{F}_x^i \\ \bar{F}_y^i \end{bmatrix} = -2 \int_0^{L/D} \int_0^{2\pi} (\bar{P}^i - 1) \begin{bmatrix} \cos(\theta) \\ \sin(\theta) \end{bmatrix} d\theta d\bar{z} \tag{2}$$

where $\bar{P}^i$ is the non-dimensional pressure distribution in bearing $i = 1, 2$. It is computed from the Narrow Groove Theory (NGT), a homogenized version of Reynold's equation assuming an infinite number of grooves [17]. The NGT simplifies the numerical treatment since the grooves do not longer need to be resolved. One would otherwise have to resort to an advanced spatial discretization scheme describing the saw-toothed waviness of the local pressure distribution caused by the periodic geometric discontinuities [18]. Omitting the superscript $(.)^i$ for the sake of clarity, and assuming an ideal gas and an isothermal compression, the NGT equation governing the gas film dynamics in a bearing writes as in [16]:

$$\begin{aligned} &\partial_\theta [\bar{P}(f_\theta \partial_\theta \bar{P} + f_c \partial_{\bar{z}} \bar{P})] + \partial_{\bar{z}} [\bar{P}(f_c \partial_\theta \bar{P} + f_z \partial_{\bar{z}} \bar{P})] \\ &+ c_s [\sin\beta \partial_\theta (\bar{P} f_s) - \cos\beta \partial_{\bar{z}} (\bar{P} f_z)] = \\ &\Lambda \partial_\theta (\bar{P} f_v) + \sigma \partial_t (\bar{P} f_v) \end{aligned} \tag{3}$$

where the f_a functions with $a = \theta, z, c, s, v$ depend on geometrical parameters and on the clearance distribution, hence on the rotor position governed by (1). This nonlinear Partial Differential Equation (PDE) is spatially defined for $(\theta, z) \in [0, 2\pi] \times [0, L/D]$ with the cyclic condition $\bar{P}(t, \theta + 2\pi, z) = \bar{P}(t, \theta, z)$. At $z = 0$ the non-dimensional pressure is set to 1 and at $z = L/D$ the mass flow normal to the bearing mid-plane interface is set to 0.

The complete set of equations governing the system's dynamics is therefore (1) coupled with two PDEs (3) to compute the aerodynamic forces (2) generated in each bearing, with the boundary conditions defined above, along with an appropriate set of initial conditions. After discretizing in space the PDEs as described hereafter, the governing equations are ultimately written under the form of a Differential Algebraic Equation (DAE) solved with the ode15s solver of Matlab [19]:

$$\begin{cases} \dot{\mathbf{y}} = \mathbf{f}(\mathbf{y}, \mathbf{y}_\Gamma, t) \\ \mathbf{0} = \mathbf{g}(\mathbf{y}, \mathbf{y}_\Gamma) \\ \mathbf{y}(0) = \mathbf{y}_0 \end{cases} \tag{4}$$

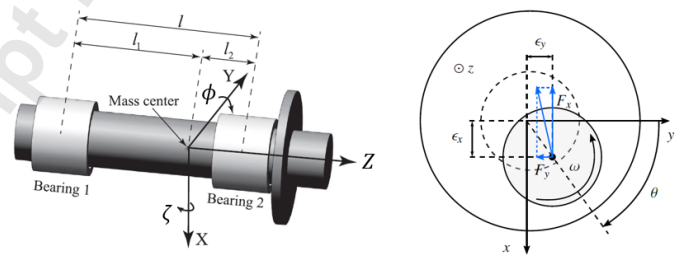

FIGURE 1: LEFT: ROTOR-BEARINGS SYSTEM, COURTESY OF [16]. RIGHT: AERODYNAMIC FORCE GENERATED IN A BEARING BY THE GAS FLOW AROUND THE ROTOR.

3. HYPER-REDUCED ORDER MODEL

3.1 Spatial discretization with finite differences

We consider the change of variable $\bar{\psi} = \bar{P} f_v$ in equation (3). A uniform rectangular grid of $n_\theta \times n_z$ nodes is used with the numbering $I(i, j) = i + (j - 1)n_\theta$, where $1 \leq i \leq n_\theta$ and $1 \leq j \leq n_z$. Given the cyclic condition at $\theta = 2\pi$, the nodal values of $\bar{\psi}$ and its partial derivatives at nodes (n_θ, j) are equal to the nodal values at nodes $(1, j)$. We then define an effective grid by removing the nodes at $i = n_\theta$ and the ones at $j = 1, n_z$ constrained by the boundary conditions. Let $\boldsymbol{\psi}$ and $\partial_a^d \boldsymbol{\psi}$ (with $a = \theta, \bar{z}$ and $d = 1, 2$) be the vectors obtained by stacking the nodal values of $\bar{\psi}$ and $\partial_a^d \bar{\psi}$ on this effective grid, respectively. Let also $\mathbf{h}_\theta$ be the $n_\theta - 1$ vector obtained by stacking the nodal values of the non-dimensional clearance distribution along the effective circumferential grid. The vector $\mathbf{h}$ of the clearance values over the complete effective grid can be recovered as $\mathbf{h} = \mathbf{B}\mathbf{h}_\theta$, with

Journal of Engineering for Gas Turbines and Power. Received August 02, 2023;
Accepted manuscript posted September 14, 2023. doi:10.1115/1.4063424

$\mathbf{B}$ an appropriate Boolean matrix. Using a central difference scheme, the discretized in space NGT equation is written as an Ordinary Differential Equation (ODE) under the form:

$$\sigma\dot{\bar{\boldsymbol{\psi}}} = -\Lambda\mathbf{A}\bar{\boldsymbol{\psi}} + c_s\sum_{i=1}^{3}\mathbf{B}u_i(\mathbf{h}_\theta).*\mathbf{C}_i\bar{\boldsymbol{\psi}} + \sum_{i=1}^{9}\mathbf{B}v_i(\mathbf{h}_\theta).*\mathbf{D}_i\bar{\boldsymbol{\psi}}.*\mathbf{E}_i\bar{\boldsymbol{\psi}} \tag{5}$$

where $\bar{\boldsymbol{\psi}} = [\bar{\psi}_{I(i,j)}]$ with $i = 1 : n_\theta - 1$ and $j = 1 : n_z$. Note that $\bar{\boldsymbol{\psi}} = [f_v(\mathbf{h}_\theta); \boldsymbol{\psi}; \boldsymbol{\psi}_\Gamma]$ with $\boldsymbol{\psi}_\Gamma$ the nodal values at the bearing mid-plane interface, that is at $j = n_z$. The u_i, v_i functions are component-wise evaluated and .* denotes the component-wise product. It can be appreciated that the above formulation distinguishes terms that are linear and quadratic in $\bar{\boldsymbol{\psi}}$, which will be exploited in the reduced order model.

3.2 Vectorized formulation

The computational cost is driven by the dimension $n = n_\theta n_z$ of the two discretized in space NGT equations (one for each bearing). To circumvent this issue, we define a single equation for $\boldsymbol{\Psi} = [\boldsymbol{\psi}^1; \boldsymbol{\psi}^2]$ that we vectorize prior applying the Galerkin projection and the sparse sampling method described in next subsection. More precisely, the idea is to rewrite the sums in (5) as matrix-vector products for which the reduction techniques apply more efficiently. This is done by using the mixt product property $\mathbf{Ax}.*\mathbf{By} = (\mathbf{A}\bullet\mathbf{B})(\mathbf{x}\otimes\mathbf{y})$, where $\otimes$ is the Kronecker product and $\bullet$ denotes the row-wise Kronecker product. Let $\mathbf{H}_\theta = [\mathbf{h}_\theta^1; \mathbf{h}_\theta^2]$ and $\bar{\boldsymbol{\Psi}} = [\bar{\boldsymbol{\psi}}^1; \bar{\boldsymbol{\psi}}^2]$. Let also $\mathbf{u}(.) = [u_1(.); u_2(.); u_3(.)]$ and similarly $\mathbf{v}(.) = [v_1(.); \ldots; v_9(.)]$. All calculations done, the vectorized equation governing $\boldsymbol{\psi}^1$ and $\boldsymbol{\psi}^2$ can be written under the form:

$$\sigma\dot{\bar{\boldsymbol{\Psi}}} = -\Lambda\boldsymbol{\mathcal{A}}\bar{\boldsymbol{\Psi}} + c_s\boldsymbol{\mathcal{F}}(\mathbf{u}(\mathbf{H}_\theta)\otimes\bar{\boldsymbol{\Psi}}) + \boldsymbol{\mathcal{G}}(\mathbf{v}(\mathbf{H}_\theta)\otimes\bar{\boldsymbol{\Psi}}\otimes\bar{\boldsymbol{\Psi}}) \tag{6}$$

where $\boldsymbol{\mathcal{A}} = \text{blkdiag}(\mathbf{A}, \mathbf{A})$ and the matrices $\boldsymbol{\mathcal{F}}, \boldsymbol{\mathcal{G}}$ are obtained from the mixt product property described above. It must be mentioned that this formulation is intractable at this point because of the high dimensional matrix-vector products involved in the equation. A similar treatment is performed on the boundary condition equations at each bearing mid-plane interface, but it is not described here for the sake of brevity.

3.3 Hyper-reduction

We first perform a Galerkin projection of equation (6) onto a reduced basis obtained with the Proper Orthogonal Decomposition (POD - [5]). This technique uses a Singular Value Decomposition (SVD) to extract the most significant uncorrelated modes of a system from a set of snapshot data. In our case, we use snapshots of the ψ distributions in each bearing to identify a reduced basis $\mathbf{V}$ of rank $r \ll 2n$ so that $\boldsymbol{\Psi} \approx \mathbf{V}\boldsymbol{\Psi}_r$. We proceed similarly to identify a reduced basis $\mathbf{V}_\Gamma$ of rank $r_\Gamma \ll 2n_\theta$ so that $\boldsymbol{\Psi}_\Gamma \approx \mathbf{V}_\Gamma\boldsymbol{\Psi}_{\Gamma r}$. Although this Galerkin projection reduces the dimension of the gas films equations, the nonlinear terms are still too expensive to evaluate. We propose to tackle them with the Discrete Empirical Interpolation Method (DEIM - [8]). This technique states that a vector-valued function may accurately be recovered from a sparse selection of its components. More precisely, given $f(.)$ a nonlinear function to be component-wise evaluated at some vector $\mathbf{x}$ of size n, the algorithm computes a reduced basis $\mathbf{V}_f$ of rank $m_f \ll n$ and inductively identifies m_f distinct entries $i_1, \cdots, i_{m_f}$, so that $f(\mathbf{x}) \approx \mathbf{V}_f f(\mathbf{P}_f^T\mathbf{x})$ with $\mathbf{P}_f^T\mathbf{x} = [x_{i_1}; ...; x_{i_{m_f}}]$. The DEIM is applied to the nonlinear functions $f_v, \mathbf{u}$ and $\mathbf{v}$ evaluated at $\mathbf{H}_\theta$. Then a reduced basis $\bar{\mathbf{V}}$ is defined using $\mathbf{V}_{f_v}, \mathbf{V}$ and $\mathbf{V}_\Gamma$ so that $\bar{\boldsymbol{\Psi}} \approx \bar{\mathbf{V}}\bar{\boldsymbol{\Psi}}_r$, with $\bar{\boldsymbol{\Psi}}_r$ a reduced vector of size $m_{f_v} + r + r_\Gamma \ll 2(n + 2n_\theta)$. All calculations done, a hyper-reduced equation governing the gas films dynamics is written under the form:

$$\sigma\dot{\bar{\boldsymbol{\Psi}}}_r = -\Lambda\boldsymbol{\mathcal{A}}_r\bar{\boldsymbol{\Psi}}_r + c_s\boldsymbol{\mathcal{F}}_r(\mathbf{u}(\mathbf{P}_\mathbf{u}^T\mathbf{H}_\theta)\otimes\bar{\boldsymbol{\Psi}}_r) + \boldsymbol{\mathcal{G}}_r(\mathbf{v}(\mathbf{P}_\mathbf{v}^T\mathbf{H}_\theta)\otimes\bar{\boldsymbol{\Psi}}_r\otimes\bar{\boldsymbol{\Psi}}_r) \tag{7}$$

with $\boldsymbol{\mathcal{A}}_r = \mathbf{V}^T\boldsymbol{\mathcal{A}}\bar{\mathbf{V}}$ and where the matrices $\boldsymbol{\mathcal{F}}_r, \boldsymbol{\mathcal{G}}_r$ are obtained using the property $\mathbf{Ax}\otimes\mathbf{By} = (\mathbf{A}\otimes\mathbf{B})(\mathbf{x}\otimes\mathbf{y})$. Again, a similar treatment is performed on the interface conditions at the bearing mid-planes. A DEIM is also performed on $f_v^{-1}(\mathbf{H}_\theta)$ to compute the pressure distributions in (2). Ultimately, it can be appreciated that the dimensions of the matrices involved in this hyper reduced order model (h-ROM) do not longer depend on the initial finite difference grid. These matrices are then computed prior the time integration allowing to significantly speed up the calculations.

4. PARAMETRIC ADAPTATION

In operational conditions, the speed of the rotor ω and the compressibility number Λ may be controlled to reach targeted performances. The reduced bases involved in the h-ROM are however obtained from snapshots of the solution computed at user-defined values of the system's parameters (training points). Accuracy is thus only expected in the neighbourhood of these training points. To circumvent this issue, we implement in this work the so-called Interpolation in the Tangent Space to the Grassmann Manifold (ITSGM - [11]). The Grassmann manifold $\mathcal{G}(n, r)$ is the set of all the r-dimensional linear subspaces of $\mathbb{R}^n$. In a projection-based model reduction framework, the range of a POD basis $\mathbf{V} \in \mathbb{R}^{n\times r}$ is then viewed as an element of $\mathcal{G}(n, r)$. Given $q \geq 2$ POD bases of rank r computed at distinct parameters, say $\mathbf{V}(\boldsymbol{\mu}_1), \cdots, \mathbf{V}(\boldsymbol{\mu}_q)$, the ITSGM method suitably outputs for a new parameter $\boldsymbol{\mu} = [\omega, \Lambda]$ a new reduced basis $\mathbf{V}(\boldsymbol{\mu})$ of rank r. Implementation-friendly formulas render this method attractive for fast reduced bases adaptation to new parameters. A comprehensive description can be found in [20]. In this work, the ITSGM method is used to adapt the reduced bases used in the Galerkin projection framework, and also to adapt the reduced bases involved in the approximation of the nonlinear terms with the DEIM method.

5. H-ROM PERFORMANCES

5.1 System parameters

The parameters of the studied system are the following: rotor mass $m_r = 0.2357$ kg, rotor radius $R = 7$ mm, rotor polar inertia $I_P = 7.8\times10^{-6}$ kg·m^2, rotor transverse inertia $I_T = 2.1775\times10^{-4}$ kg·m^2, groove width ratio $\alpha = 0.65$, groove angle $\beta = 19°$, clearance at null eccentricity $h_{r0} = 4.5$ μm, groove depth $\delta = 10$

Journal of Engineering for Gas Turbines and Power. Received August 02, 2023;
Accepted manuscript posted September 14, 2023. doi:10.1115/1.4063424

μm, bearing length on diameter $L/D = 1$. The rotor-bearings system is operated in air with a viscosity $\mu = 1.95 \times 10^{-5}$ Pa and the gravity constant is set to $g = 9.81$ m·s^{-2}. The radial growth of the rotor due to the high rotation speed is taken into account with the following formula:

$$r_g = \frac{1-\nu}{4E}\rho\omega^2 R^3 \tag{8}$$

with the material parameters $E = 593$ GPa, $\rho = 14500$ kg/m^3 and $\nu = 0.22$. The imbalance forces and moments computed in subsection 5.5 use the following parameters defined in [16]: $l_1 = 0.0248$ m, $U_1 = 3\times10^{-8}$ kg·m, $l_2 = 0.0207$ m, $U_2 = 3\times10^{-8}$ kg·m. All the calculations are performed with Matlab R2022b on a laptop with a single Intel(R) Core(TM) i7-7600U 2.80GHz CPU 16Go RAM.

The initial conditions used for the time integration of the governing equations are computed as follows. For a given rotation speed and compressibility number, the steady state of the dynamical system is computed by zeroing the time derivative and the imbalance forces and moments in the governing equations (4). The initial state $\mathbf{y}_0$ is then set equal to the steady state except the state variables corresponding to the initial rotor position that are modified.

5.2 h-ROM parameters and test points

The h-ROM reduced bases are computed for 9 sets of parameters on the tensor grid $[\omega_i, \Lambda_j] \in \{50, 100, 150\}$krpm $\times \{10, 25, 50\}$ (training points) . Let $\boldsymbol{\epsilon}_0 = [\epsilon_x(0), \epsilon_y(0), \zeta(0), \phi(0)]$ denote the perturbed rotor position used in the initial conditions. For each training point, the reduced bases are obtained from snapshots of the solution of equation (4) computed on a time interval of 20 rotor revolutions, with 50 time steps per revolution, and with an initial rotor position $\boldsymbol{\epsilon}_0 = [0; 0; 0; 0]$. The ranks used for $\mathbf{V}$ and $\mathbf{V}_\Gamma$ are 26 and 16, respectively, and the ranks used for the DEIM approximations of $f_v(\mathbf{H}_\theta), \mathbf{u}(\mathbf{H}_\theta)$ and $\mathbf{v}(\mathbf{H}_\theta)$ are 6, 16 and 30, respectively. The performances of the h-ROM are studied on the four following sets of simulation parameters, see Figure 2:

#1: $\omega = 100$krpm, $\Lambda = 25$, $\boldsymbol{\epsilon}_0 = [0; 0; 0; 0]$ (training point)

#2: $\omega = 100$krpm, $\Lambda = 25$, $\boldsymbol{\epsilon}_0 = [0.2; 0.2; 3°; -3°]$ (test point)

#3: $\omega = 87$krpm, $\Lambda = 38$, $\boldsymbol{\epsilon}_0 = [0; 0; 0; 0]$ (test point)

#4: $\omega = 87$krpm, $\Lambda = 38$, $\boldsymbol{\epsilon}_0 = [0.2; 0.2; 3°; -3°]$ (test point)

The h-ROM solutions are compared to the Full Order Model (FOM) solutions, that is to the numerical solutions of (4) obtained without using the reduction techniques. We focus in this study on the rotor orbit predictions $[\epsilon_x^i(t), \epsilon_y^i(t)]$ in each bearing on a time interval of 20 rotor revolutions with a relative error indicator based on the Frobenius norm.

5.3 Stability analysis

We first perform a stability analysis to check if the system can be safely operated for any $[\omega, \Lambda] \in$ [50,150]krpm×[10,50]. We proceed as in [13] by studying the sign of the real part of the leading eigenvalue of the Jacobian of the dynamical system (4). The latter is numerically computed for different values of the rotor speed and of the compressibility number, and the highest real part of its eigenvalues is reported in Figure 3. Except for rotation speeds higher than 130krpm at $\Lambda = 50$, the real part of the leading eigenvalue remains negative. The dynamical system is then stable outside this range in the linear sense, that is without external forces or imbalance the rotor will come back to its steady state position after any slight perturbation.

5.4 Mesh sensitivity

Figures 4 and 5 show the influence of the mesh on the h-ROM and FOM solutions computed with the set #1 of simulation parameters (100krpm) without taking into account the imbalance forces and moments. The h-ROM predictions are in close agreement with their FOM counterparts, with a relative error lower than 1% for the rotor orbits in each bearing, see Table 1. The speeding up factor obtained on the time integration of the h-ROM compared to the FOM ranges from 4 with the 20-by-20 mesh to almost 400 with the 60-by-60 mesh. This important speeding up factor obtained by refining the mesh is the consequence of using reduced matrices that do not depend on the grid. It is however important to mention that the cost for computing the h-ROM matrices prior the time integration scales with the number of grid points. In addition, given the errors committed for test points far from the training points, see subsection 5.5, it is sufficient to use the 40-by-40 mesh.

Grid	20×20	40×40	60×60
Bearing 1	0.0576%	0.429%	0.273%
Bearing 2	0.0473%	0.391%	0.271%
Speeding up	×4	×50	×391

TABLE 1: ERROR H-ROM/FOM DEPENDING ON THE MESH AND SPEEDING UP FACTOR FOR THE TIME INTEGRATION (SET OF SIMULATION PARAMETERS #1).

5.5 Accuracy analysis on test points

Finally, we explore the accuracy of the h-ROM on test points #1 to #4 considering the imbalance forces and moments. A 40-by-40 grid is used for each bearing. As illustrated on Figure 2, test points #2,3,4 differ from the 9 training points by the values of the rotation speed, the compressibility number, or the initial rotor position. We use the ITSGM method described in section 4 to adapt the reduced bases of the h-ROM with respect to the rotation speed and the compressibility number only, and we investigate the extrapolation performances of the h-ROM for new values of the initial rotor position (test points #2 and #4).

Table 2 presents the h-ROM performances in terms of relative error and speed up factor with respect to the FOM. As expected, the error is the lowest (0.06%) at test point #1 which coincides with a training point. Figure 6 illustrates the close agreement between the h-ROM and FOM solutions. In addition, it is observed that the error increases as the test point is moved away from the training points, with a higher sensitivity when changing the rotor speed and the compressibility number than when changing the initial rotor position. Indeed, test point #2

Journal of Engineering for Gas Turbines and Power. Received August 02, 2023;
Accepted manuscript posted September 14, 2023. doi:10.1115/1.4063424

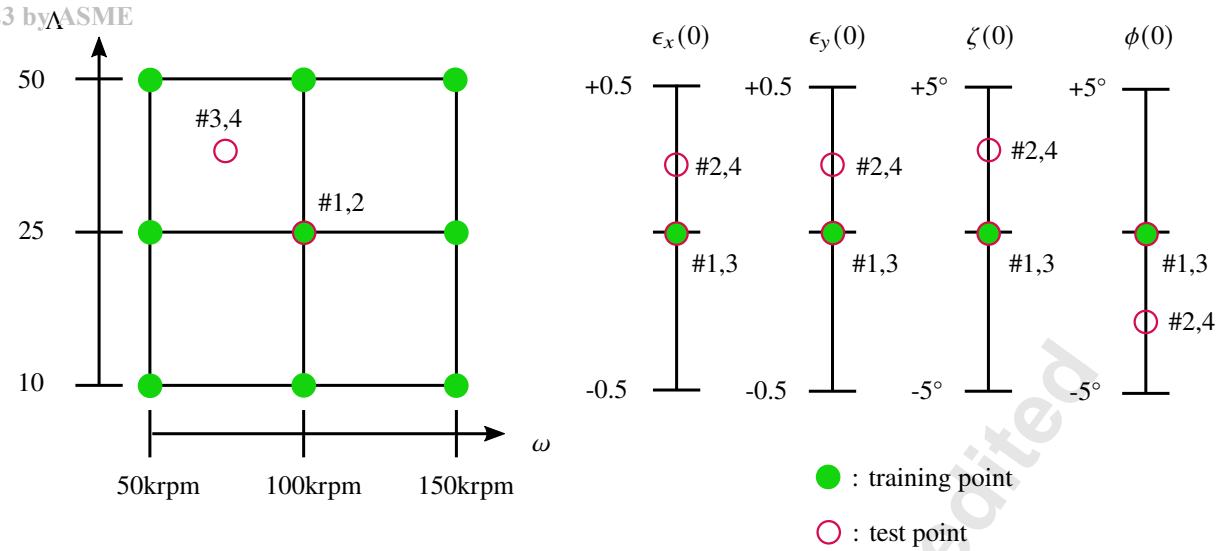

FIGURE 2: TRAINING POINTS AND TEST POINTS IN THE PARAMETER SPACE

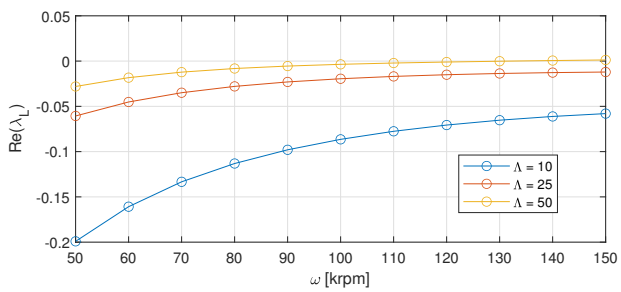

FIGURE 3: REAL PART OF THE LEADING EIGENVALUE DEPENDING ON THE ROTOR SPEED AND THE COMPRESSIBILITY NUMBER

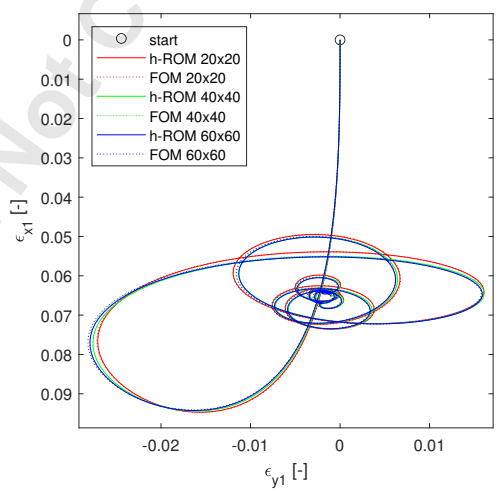

FIGURE 4: H-ROM AND FOM PREDICTIONS DEPENDING ON THE MESH (SET #1 OF SIMULATION PARAMETERS).

differs from test point #1 by the initial rotor position only, and the error is 1.1%; while test point #3 differs from test point #1 by the rotor speed and the compressibility number, and the error reaches 11.6%. Test point #4 confirms that changing the initial rotor position does not significantly change the accuracy, as the error difference between test points #3 and #4, which only differ by the initial rotor position, is 0.4%. This confirms that it is sufficient to adapt the reduced bases with respect to the rotor speed and the compressibility number only, as performed in this study, and not with respect to the initial rotor position. Last, we notice that for all the simulations the h-ROM computes the solution much faster than the FOM, with a speed up factor ranging from 40 to 100 depending on the test point, with relative errors lower than 12%. This study suggests that the developed h-ROM is both accurate and efficient even far from the training points. Figure 7 displays the simulation results for test point #4, showing that an error level of 12% remains satisfactory.

6. LIMITATIONS

The objective of a hyper-reduced order model (h-ROM) framework is to approximate the behavior of a complex dynamical system with fewer degrees of freedom, by reducing the dimensionality of the governing equations while retaining the essential features. However, this framework has a number of limitations, especially for gas-bearings supported rotor systems, that must be mentioned. First, as commonly observed with projection-based model order reduction techniques, the h-ROM may not capture the system's behavior accurately if the ranks of the reduced bases are too small. It is therefore important to verify the accuracy obtained with the selected ranks by comparing the results of the h-ROM to those of the FOM for different values of the system's parameters. Second, the developed h-ROM is designed to work for a specific set of governing equations. Hence it may not be easily adaptable to flexible rotor models or to other types of gas bearing technologies such as foil bearings. A dedicated study should be conducted for any change in the governing equations to verify if the reduction techniques employed in this study are

Journal of Engineering for Gas Turbines and Power. Received August 02, 2023;
Accepted manuscript posted September 14, 2023. doi:10.1115/1.4063424

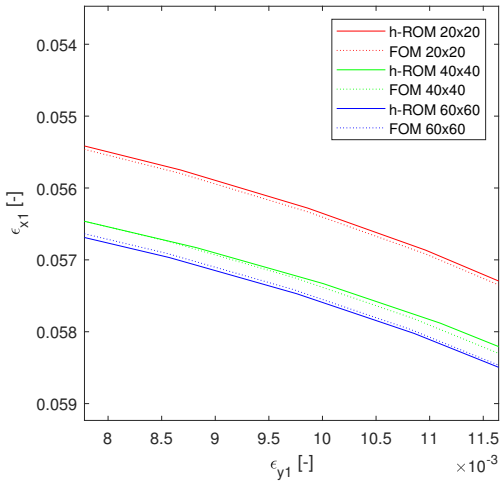

FIGURE 5: ZOOM ON THE H-ROM AND FOM PREDICTIONS DEPENDING ON THE MESH (SET #1 OF SIMULATION PARAMETERS).

Test point	#1	#2	#3	#4
Bearing 1	0.0638%	1.25%	11.1%	11.5%
Bearing 2	0.0640%	1.10%	11.6%	12.0%
Speeding up	×40	×66	×86	×101

TABLE 2: ERROR AND SPEED UP FACTOR H-ROM/FOM DEPENDING ON THE SET OF SIMULATION PARAMETERS.

applicable for the considered system. However, the developed h-ROM could more easily adapt to different loading scenarios, such as a shock applied to the rotor or a forced vibration, by computing the reduced bases with snapshots of the FOM associated to these different scenarios. Last, this h-ROM framework may fail to describe highly nonlinear behaviors such as bifurcations. This situation may be encountered if the rotor is operated near or beyond the so-called onset speed of instability (OSI). In this situation, it might be necessary to cluster the parameter space accordingly and to use separate sets of reduced bases, or to use another reduction approach able to capture such behavior.

7. CONCLUSION

We presented in this study the hyper-reduced order model (h-ROM) of a gas-bearings supported rotor. The developed h-ROM is parametric and efficiently adapts to changes in both the rotor speed and the compressibility number. Numerical experiments demonstrate that the h-ROM speeds up the calculations up to two orders of magnitude with relative errors lower than 10% compared to a high fidelity model. This parametric surrogate model will be used in future works in the digital twin of a small-scale high-speed turbomachinery for anomaly detection.

ACKNOWLEDGMENTS

This work was supported by the Center for Intelligent Systems of the École Polytechnique Fédérale de Lausanne. The first author would like to thank the EPFL Master students who helped in the numerical study of the dynamical system: Mr Philipp Weder and Mr David Nikravech.

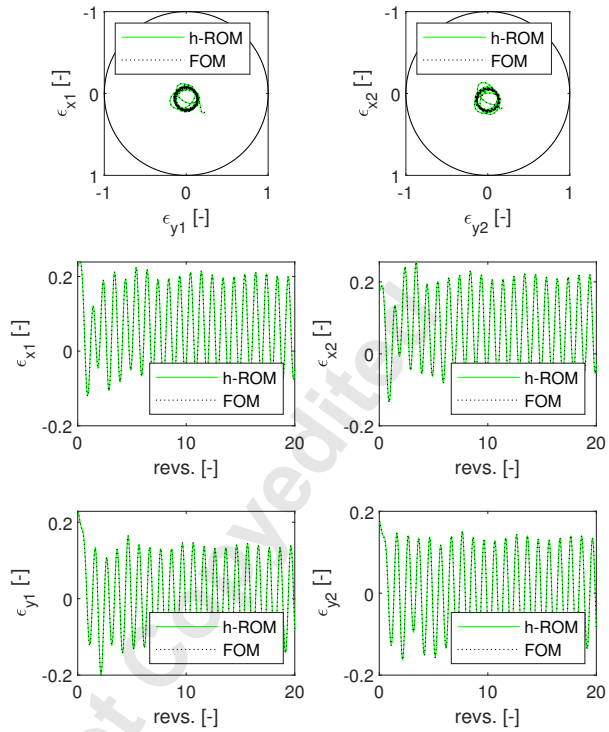

FIGURE 6: PREDICTIONS FOR THE SET #2 OF SIMULATION PARAMETERS.

REFERENCES

[1] Heng, Aiwina, Zhang, Sheng, Tan, Andy CC and Mathew, Joseph. "Rotating machinery prognostics: State of the art, challenges and opportunities." *Mechanical systems and signal processing* Vol. 23 No. 3 (2009): pp. 724–739.

[2] Chinesta, Francisco, Cueto, Elias, Abisset-Chavanne, Emmanuelle, Duval, Jean Louis and Khaldi, Fouad El. "Virtual, digital and hybrid twins: a new paradigm in data-based engineering and engineered data." *Archives of computational methods in engineering* Vol. 27 No. 1 (2020): pp. 105–134.

[3] Benner, Peter, Gugercin, Serkan and Willcox, Karen. "A survey of projection-based model reduction methods for parametric dynamical systems." *SIAM review* Vol. 57 No. 4 (2015): pp. 483–531.

[4] Sirovich, L. "Turbulence and the dynamics of coherent structures, Parts I, II and III." *Quart. Appl. Math.* (1987): pp. 561–590.

[5] Rathinam, Muruhan and Petzold, Linda R. "A new look at proper orthogonal decomposition." *SIAM Journal on Numerical Analysis* Vol. 41 No. 5 (2003): pp. 1893–1925.

[6] Astrid, Patricia, Weiland, Siep, Willcox, Karen and Backx, Ton. "Missing point estimation in models described by proper orthogonal decomposition." *IEEE Transactions on Automatic Control* Vol. 53 No. 10 (2008): pp. 2237–2251.

[7] Carlberg, Kevin, Farhat, Charbel, Cortial, Julien and Amsallem, David. "The GNAT method for nonlinear model

Journal of Engineering for Gas Turbines and Power. Received August 02, 2023;
Accepted manuscript posted September 14, 2023. doi:10.1115/1.4063424

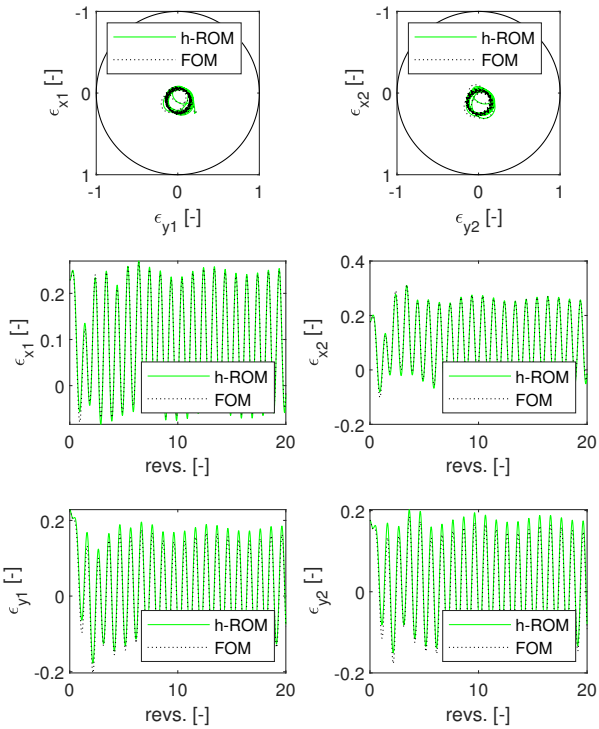

FIGURE 7: PREDICTIONS FOR THE SET #4 OF SIMULATION PARAMETERS.

reduction: effective implementation and application to computational fluid dynamics and turbulent flows." *Journal of Computational Physics* Vol. 242 (2013): pp. 623–647.

[8] Chaturantabut, Saifon and Sorensen, Danny C. "Nonlinear model reduction via discrete empirical interpolation." *SIAM Journal on Scientific Computing* Vol. 32 No. 5 (2010): pp. 2737–2764.

[9] Washabaugh, Kyle, Amsallem, David, Zahr, Matthew and Farhat, Charbel. "Nonlinear model reduction for CFD problems using local reduced-order bases." *42nd AIAA Fluid Dynamics Conference and Exhibit*: p. 2686. 2012.

[10] Peherstorfer, Benjamin, Butnaru, Daniel, Willcox, Karen and Bungartz, Hans-Joachim. "Localized discrete empirical interpolation method." *SIAM Journal on Scientific Computing* Vol. 36 No. 1 (2014): pp. A168–A192.

[11] Amsallem, David, Cortial, Julien, Carlberg, Kevin and Farhat, Charbel. "A method for interpolating on manifolds structural dynamics reduced-order models." *International journal for numerical methods in engineering* Vol. 80 No. 9 (2009): pp. 1241–1258.

[12] Mosquera, Rolando, Hamdouni, Aziz, El Hamidi, Abdallah and Allery, Cyrille. "POD basis interpolation via Inverse Distance Weighting on Grassmann manifolds." *Discrete & Continuous Dynamical Systems-S* Vol. 12 No. 6 (2019): p. 1743.

[13] Bonello, Philip and Pham, Hai Minh. "The efficient computation of the nonlinear dynamic response of a foil–air bearing rotor system." *Journal of Sound and Vibration* Vol. 333 No. 15 (2014): pp. 3459–3478.

[14] Cherabi, Bilal, Hamrani, Abderrachid, Belaidi, Idir, Khelladi, Sofiane and Bakir, Farid. "An efficient reduced-order method with PGD for solving journal bearing hydrodynamic lubrication problems." *Comptes Rendus Mécanique* Vol. 344 No. 10 (2016): pp. 689–714.

[15] Iseli, Elia, Guenat, Eliott, Tresch, Roger and Schiffmann, Jürg. "Analysis of spiral-grooved gas journal bearings by the narrow-groove theory and the finite element method at large eccentricities." *Journal of Tribology* Vol. 142 No. 4 (2020).

[16] Liu, Wanhui, Bättig, Philipp, Wagner, Patrick H and Schiffmann, Jürg. "Nonlinear study on a rigid rotor supported by herringbone grooved gas bearings: Theory and validation." *Mechanical Systems and Signal Processing* Vol. 146 (2021): p. 106983.

[17] Vohr, John H and Chow, CY. "Characteristics of herringbone-grooved, gas-lubricated journal bearings." (1965).

[18] Bonneau, D and Absi, J. "Analysis of aerodynamic journal bearings with small number of herringbone grooves by finite element method." *ASME. J. Tribol.* Vol. 116 No. 4 (1994): pp. 698—-704.

[19] Shampine, Lawrence F and Reichelt, Mark W. "The matlab ode suite." *SIAM journal on scientific computing* Vol. 18 No. 1 (1997): pp. 1–22.

[20] Zimmermann, Ralf. "Hermite interpolation and data processing errors on Riemannian matrix manifolds." *SIAM Journal on Scientific Computing* Vol. 42 No. 5 (2020): pp. A2593–A2619.